Solid Freeform Fabrication 2023: Proceedings of the 34th Annual International Solid Freeform Fabrication Symposium – An Additive Manufacturing Conference
Reviewed Paper

Fiber-Reinforcement of Binder-Jetted Casting Molds for Multiple Usage

J. Angenoorth*, D. Rumschöttel*, B. Leitner†, V. Schumm†, F. Ettemeyer*, I. Ünsal†, and D. Günther*

*Fraunhofer Institute for Casting, Composite and Processing Technology, IGCV, Garching, Germany 85748
†Fraunhofer Institute for Casting, Composite and Processing Technology, IGCV, Augsburg, Germany 86159

Abstract

Widely used sand casting with lost molds is an efficient and cost-effective way of producing geometrically complex components. As the demand for sand has tripled over the last two decades, finding new solutions for thermostable binder systems and ensuring the efficient use of resources is essential. To address this issue, the REINFORCED SAND project is exploring glass fiber-reinforced sand molds and temperature-stable inorganic binders within the binder-jetting process. The aim is to improve the mechanical properties of the 3D-printed casting molds to make multiple uses of these possible, reducing resource consumption and increasing profitability. For this purpose, various material systems and manufacturing parameters were examined. It has been demonstrated that fiber-reinforced sand molds can be used for multiple castings, and fibers can be principally processed in the binder jetting process. These efforts aim to make sand casting production more environmentally friendly and sustainable. The REINFORCED SAND project is a step towards achieving these goals.

Introduction

The casting technology, compared to other manufacturing processes, enables cost-efficient production of highly geometrically complex and function-integrated parts obeying the following process steps:

- The mold halves and cores define the cast.
- The casting mold is assembled with these mold halves and cores.
- Subsequently, the part is cast, cooled down, and removed from the mold.
- Finally, the cores are removed with the help of mechanical or chemical processes and machined if necessary.

Mass production with a large capacity typically involves the use of permanent molds, usually made from metal. Prototypes and small to middle production mostly use the sand casting process, where the molds and cores are only used once [1]. This leads to high resource consumption and a challenging recycling process due to organic or inorganic sand mold additives [2]. The demand for sand has tripled to 40 to 50 billion metric tons per year in the past two decades, and sand is the second most traded resource in the world after water [3]. Despite the large resource deposit, it is desirable to guarantee resource-saving via further processing and reprocessing. To create an environmentally friendly and sustained production chain in sand casting, new solutions are required for the binder systems and to integrate an efficient use of resources through reusable casting molds.

The aim of reinforcing sand molds for the casting industry with fibers is to find a middle ground between the immense investment for permanent molds and the single-use of sand molds. Incorporating fibers into the sand molds is anticipated to improve the mechanical characteristics of the disposable molds and cores, preventing the degradation of the fiber-reinforced molds, and enabling their reuse.

Furthermore, sand cores enable the production of highly complex internal structures. These cores also consist of a mold base material and a binder that connects the mold base material. Due to their micromechanical structure, sand cores exhibit highly brittle failure behavior. Because of this behavior, sand cores hardly undergo any plastic deformation and disintegrate immediately. This can particularly be a challenge for handling processes, as the sand cores fail brittly when overloaded and can bring automated production to a hault, as the brittly failed sand cores disintegrate into many fragments and cannot be removed as a whole from the process chain by a robot when a defect is detected in the core.

The fibers in the molding material that absorb the deformation energy may shift the highly brittle failure behavior of sand molds and cores into a ductile material behavior. Further, an inorganic binder is used in order to minimize harmful combustion gases to the environment and health that emerge from decomposing organic binder i.e. furan and phenolic resin [4].

State of the Art

Sand Cores and Sand Forms in Casting Industry

Sand cores are often used to produce highly complex internal structures in cast components. These are usually made from a mold base material such as silica sand and a binder with chemical additives. Due to increased environmental requirements, inorganic binders based on water glass are increasingly being used. In the industrial environment, sand cores are produced either by core shooting or binder jetting. In both processes, the mold base material is mixed with binder and additives and, in the case of inorganic binder systems, the sand-binder system is then solidified by drying the liquid binder phase.

Mechanical Properties of Sand Cores

In industry, minimum tensile strengths between 2.7 and 3.3 MPa are usually required for sand cores [5]. Due to their structure, sand cores have a porous microstructure and can be classified as granular media. These exhibit a pressure-dependent material behavior and thus endure significantly more compressive loads compared to tensile loads. The mechanical properties of sand cores are often characterized in the foundry industry using bending bars [5,6]. The bending strength was measured from breaking the bars in bending tests. Sand cores exhibit brittle failure and typical elastic moduli between 6 and 8 GPa. Lechner et. al. [7] were able to demonstrate the highly brittle strain behavior with microstructural cracking before macroscopic visibility optically.

Fiber Reinforcement of powder based materials in different fields of use

Fiber reinforcement of brittle materials is also used in the field of construction materials. In this process, the properties of concrete are improved by adding fibers made of glass, minerals, metals or polymers [8]. Fiber-reinforced concrete (FRC) has improved crack resistance and energy absorption capacity compared to normal concrete [9]. This is practically used in the field of earthquake resistance [10] or splinter protection in the event of explosions [11] or fire [12]. Shrinkage cracks occurring during the curing of concrete can also be reduced by fiber reinforcement [13].

In all the aforementioned applications, fiber reinforcement achieves only a slight improvement in strength before the first cracks occur, i.e., in the first part of the stress-strain curve up to the first maximum, there is only a slight difference compared to unreinforced concrete. The benefit of fiber-reinforced concrete becomes evident after the initial crack forms. Unlike purely brittle materials that abruptly lose strength, the fibers help hold the material together even after cracking, allowing the force to continue being transferred. This property is similar to the behavior of ductile materials, in which plastic deformation occurs when overstressed, but the material is not spontaneously destroyed. For this reason, we will refer to this fracture behavior as quasi-ductile throughout the paper.

Eldesouky et. al. [14] showed that randomly distributed fiber reinforcement of dry sand can increase the shear strength and dilation of sand, which could be used for soil stabilization. An investigation was conducted on the use of fiber reinforcement with polypropylene fiber, aluminum silicate fiber, and glass fiber in a liquid water glass binder for investment casting. To increase the strength of inorganically bonded investment casting molds, Lü et al. [15] mixed various fibers into the mold material and determined the green strength, firing strength, and residual strength of these fiber-reinforced shells. It could be shown that the bending strength of green shell specimens in investment casting can be already increased with a 0.6 wt.% content of fibers [16].

Materials and Methods

Specimen Production

The process for the production of test specimens is shown in *Figure 1*. The test specimens used are rectangular bending bars similar to those commonly used in the foundry industry [6,17]. The specimens have a length of 170 mm and a cross section of 22.4 × 22.4 mm². To produce the test specimens, a mold base material (Quartz sand GS14RP, *Strobel Quarzsand GmbH*) with an average grain diameter of 130 µm is stirred in a mixer (EUROSTAR 100 control, *IKA®-Werke GmbH & CO. KG*) with the addition of liquid water glass binder (IOB binder, *voxeljet AG*) at a speed between 350 and 500 rpm for a maximum of five minutes. This speed was chosen based on experience, as the best mixing was observed at these speeds.

Different glass fiber (GF) types (overview in *Table 1*) and lengths are mixed together with the mold base material and the liquid water glass binder until all components are wetted as well as possible. The goal was to achieve a homogeneous mixture of fiber-binder mixture with the added fibers.

GF 1 (alkali resistant glass fiber designed for concrete applications) and GF 6 (glass fiber designed for gypsum or wet-laid processes) are glass fibers commonly used in inorganic binder systems, which is why they were chosen. GF 2 and GF 3, both glass fibers designed for use with organic binder resins, were also tested using the liquid water glass binder.

To test the influence of fiber surface coating on the miscibility of fibers in the sand-binder system, an uncoated glass fiber GF 4 was chosen. The uncoated glass fiber used is a standard alkali-free E-glass fiber with a diameter of 16 µm, which is one of the most widely used types of glass fiber worldwide.

To reach the lower limit of the fiber length range, ground fibers with a length of 200 µm were also tested.

To test the recyclability the recycled E-glass fiber GF 7 with a diameter of about 15 µm was chosen. It is coming from a two-step pyrolysis process. The first step is a pyrolysis step under nitrogen atmosphere and the second step an oxidation step under synthetic air with 20 % oxygen to remove char from the surface of the fiber. The fibers were reclaimed from an UP/PMMA-resin composite at 500 – 550 °C. This fiber was chosen to investigate the influence of the recycling process on the mechanical properties of the fiber-reinforced material.

The mixing time required for a homogeneous mixture is indicated in Table 2.

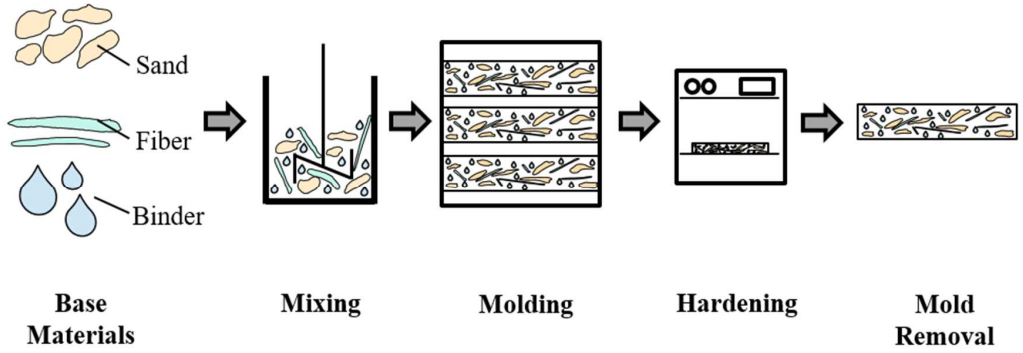

Figure 1: Process chain for specimen production

For every bending bar approximately 135 g of sand-binder-fiber mixture was stamped into a steel mold and afterwards cured in a furnace at 80 °C for 1.5 h, except for GF 7, where 200 °C was used according to [18]. After removing the mold, the bending bar specimens can be used for mechanical testing.

Table 1: Reinforcing materials – an overview

Short name	Fiber type	Fiber length	Manufacturer
GF 1	CEM-FIL 5325 AR Direct Roving	6.3 mm	Owens Corning
GF 2	Advantex SE-3030-24-4800	4.2 mm, 6.3 mm, 16.8 mm	3b fibreglass
GF 3	Advantex 399A-AP-2400	6.3 mm	3b fibreglass
GF 4	GF uncoated	16.8 mm	Standard E-glass fiber without surface coating
GF 5	GF milled	200 µm	R&G
GF 6	Advantex Wet Used Chopped Strand WS 6050-16	6 mm	3b fibreglass
GF 7	Recycled glass fiber from pyrolysis process	6 mm, 12 mm	Fraunhofer IGCV

Within the experimental design the binder quantity, fiber type, fiber content and fiber lengths are varied, see *Table 2*. Five bending bars were produced for each experiment.

Table 2: Experimental design.

Experiment number	Fiber type	Fiber length in mm	Amount of fibers in wt.%	Amount of Binder in wt.%	Mixing Time in minutes
GF1_1	GF 1	6.3	0.5	3.5	15
GF2_1	GF 2	6.3	0.5	3.5	15
GF2_2	GF 2	6.3	1	3.5	15
GF2_3	GF 2	6.3	2.5	3.5	15
GF2_4	GF 2	6.3	3.75	3.5	15
GF2_5	GF 2	6.3	5	3.5	15
GF2_6	GF 2	6.3	7	3.5	15
GF2_7	GF 2	4.2	2.5	3.5	15
GF2_8	GF 2	16.8	2.5	3.5	10[1]
GF2_9	GF 2	6.3	2.5	7	15
GF2_10	GF 2	6.3	2.5	14	15
GF3_1	GF 3	6.3	5	3.5	15
GF4_1	GF 4	16.8	2.5	3.5	10[1]
GF4_2	GF 4	4.2	2.5	3.5	15
GF4_3	GF 4	6.3	5	3.5	15
GF5_1	GF 5	0.2	1	3.5	5
GF5_2	GF 5	0.2	2	3.5	5
GF5_3	GF 5	0.2	5	3.5	5
GF6_1	GF 6	6	2.5	3.5	5
GF6_2	GF 6	6	5	3.5	5
GF7_1	GF 7	6	5	3.5	5
GF7_2	GF 7	12	5	3.5	5

[1] Manually mixed into the sand-binder mixture.

Mold Production and Casting

To test the fiber reinforced molding material in the casting process, a mold in the shape of a knight chess figure – as can be seen in *Figure 2* – was selected. This shape was chosen because of its sophisticated shape and the amount of detail that allows to make a statement about the surface quality. The maximum height of the figure from the socket to the top of the head is 75 mm, and it has a maximum width of 50 mm. The mold base material was stirred in a mixer with a whisk attachment with the addition of liquid water glass binder at a speed level three for 60 seconds. GF 2, the glass fiber type that yielded the best results in the “Specimen Production” chapter, was continuously added in small amounts within 1 minute of continuous stirring to prevent fiber agglomeration. Subsequently, the sand-binder-fiber system was pressed into an aluminum mold with the positive chess-figure model fixed in the mold. Afterwards, the mold was cured in an oven at 200 °C for two hours. In parallel, a reference casting mold without any fiber content was also produced for each fiber-reinforced casting mold with different fiber ratios to ensure comparability. In addition to each mold, five bending bars – as described in the chapter "Specimen Production" – were made from the same batch for comparison purposes. Three different GF 2 fiber fractions, each with 3 wt.%, 5 wt.%, and 7 wt.% were investigated.

The molds were then cast with a standard AlSi-alloy at 680 °C and tested for reusability. If the mold had not been destroyed during casting and demolding, another casting attempt was made. This process was repeated until the mold was destroyed.

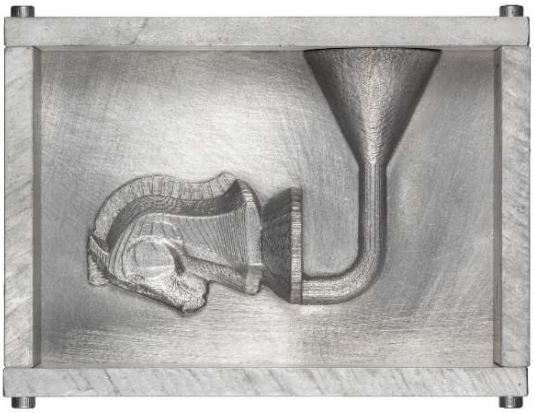

Figure 2: Aluminum mold with a model of a knight chess figure for the production of sand casting molds.

Binder-Jetting of Fiber-reinforced Bending Bars

To test the general processability of glass fibers in 3D-printing, bending bars – as described in the chapter “Specimen production” – were produced on two different 3D-printing systems. In these experiments, the processability of the GF 2 fibers was the primary focus; hence, the quantity of fibers introduced had not been examined initially. Bending bars were printed along the coating direction. The coating mechanism and binder system were investigated in relation to fiber reinforcement. The production of bending bars using the Binder Jetting method involves the following process steps: first, a layer of sand is deposited and leveled. Then, a binder agent is printed onto the leveled sand layer. The material solidifies at the locations where binder material is applied in a subsequent chemical step. The fibers were evenly spread manually using a 1 mm mesh sieve for 5 seconds per printed bending bar layer at a height of approximately l5 cm. The bending bars were placed 5 cm apart along the long side in the transverse direction within the build chamber. The process starts again, and sand is applied onto the printed and fiber-scattered layer. This process is repeated layer by layer, creating a sand bed in which the desired object is located. After the curing process, the component is removed from the sand bed with full strength. This process is schematically shown in *Figure 3*.

Coating a sand-fiber mixture proved to be impossible in a preliminary test. Firstly, due to electrostatic charging, fiber can hardly be mixed with dry sand. Secondly, the fibers block the narrow coating gap of the coater, making homogenous coating impossible.

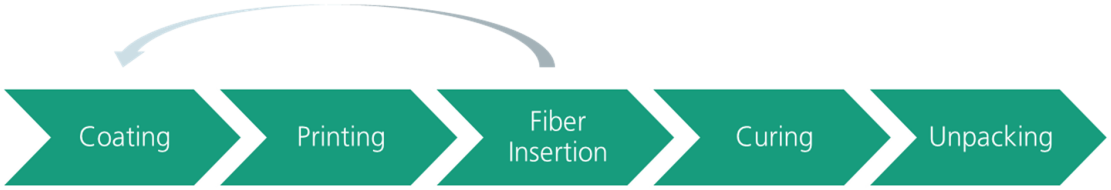

Figure 3: Process of the Binder-Jetting method. The process steps "Coating" and "Printing" are repeated until the desired object is completely printed.

Two binder systems were tested. The first one is a two-component system consisting of furan resin and an activator (RPT 2, *voxeljet AG*) – an acid – which is mixed into the sand prior to 3D printing. In this system, 3 wt.% of furan resin was printed into the sand with 0.3 wt.% content of activator. Using the binder system, four bending bars (two with fiber reinforcement and two reference bars without fiber addition) were printed on a prototype in-house research 3D printer with a layer height of 350 micrometers in the coating direction. In this case, the coating module consists of a sand dispenser that sprinkles sand onto the previous layer and a counter rotating roller, smoothing and compressing the previously deposited sand layer. This process is shown in the schematic diagram of *Figure 4*.

The second binder, a single component water glass (IOB, *voxeljet AG*), was used in the voxeljet VX1000 printer with a 3 wt.% binder content. Using this binder system, six bending bars (three with fiber reinforcement and three reference bending bars without fiber addition) were printed with a layer height of 350 micrometers in the coating direction. The coating module consists of a blade that smoothes and compresses the previously applied sand and a sand dispenser located directly above the blade. In this case, sand is not sprinkled onto the glass fibers but pushed over the fiber layer.

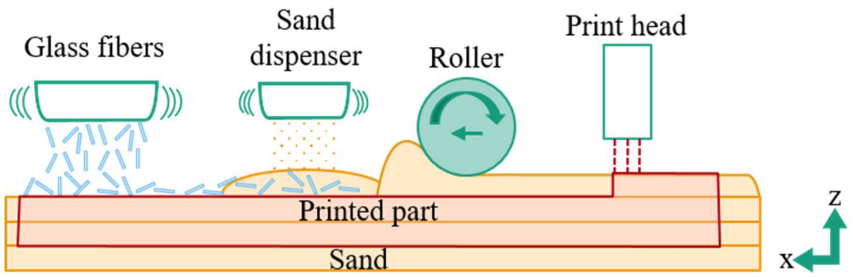

Figure 4: Schematic diagram of the 3D-printing process with help of a roller coater, used for the organic binder system.

3-Point-Bending Test

All specimens are tested by a 3-point-bending test on a universal testing machine (Z050, *ZwickRoell GmbH & Co. KG*) with a 1 kN load cell. The support has a distance of 150 mm, and the load is induced in the middle of the bending bar. Both the supports and the stamp have radii of 5 mm. The test is carried out with a test speed of 5 mm/min. On the bottom of the specimen, a length gauge is installed to measure the bending distance of the specimen (3-P bending feeler 211 mm with makroXtens). With the 3-point-bending test, the strength of the specimens as well as the elongation at break is measured, shown in Figure 5, where F is the applied force, L_{3P} is the distance between the two supports, I_{3P} is the length of the specimen, h_{3P} is the height, and w_{3P} the width of the specimen.

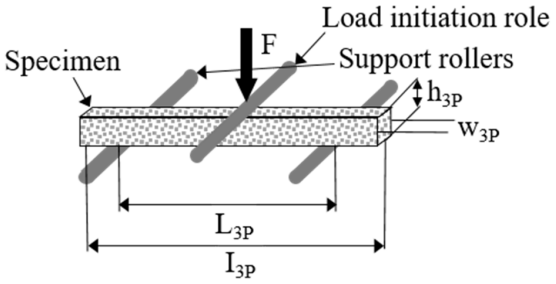

Figure 5: Schematic diagram of the 3-point-bending test [19].

GOM

The GOM ATOS Compact Scan (*Carl Zeiss GOM Metrology GmbH*) with the MV170 attachment was used to determine and compare the castings' surface with a measuring volume of 170 x 130 mm², a camera angle of 27.1°, and a camera resolution of 12 megapixels.

The open-source software CloudCompare (*cloudcompare.org*) was used to generate a point cloud and calculate the average absolute deviation (AAD) between the castings and the ideal CAD model. The AAD was calculated using Equation 1, where n is the number of measured points, and x_i is the deviation from the measured point to its corresponding point with the minimum distance on the ideal CAD model. The first, fifth, and tenth castings were compared, produced using the mold with 5 wt.% and 7 wt.% GF 2, along with their respective reference castings.

$$\frac{1}{n}\sum_{i=1}^{n}|x_i| \qquad \textit{Equation 1}$$

Results

Specimen Production

The specimens were produced with different glass fibers, different fiber lengths and different amount of glass fiber and binder in the mixture and were tested with a 3-point-bending test. Here, the bending strength and the deflection were evaluated and are shown in the following *Table 3*. It was found that some glass fibers and their blends with sand and binder result in much higher elongation at break at maximum force than the elongation at break at maximum force without glass fiber reinforcement. The breaking behavior changed from brittle behavior to a more quasi-ductile breaking behavior, see *Figure 6*.

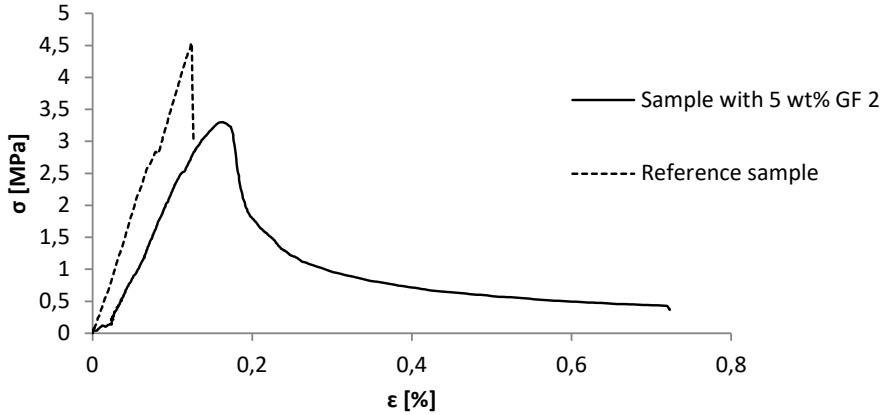

Figure 6: Example of breaking behavior of a sample without glass fiber reinforcement and a sample of GF 2 with 5 wt.% of glass fiber. It can be seen that the unreinforced specimen (dotted line) shows a brittle fracture behavior, while the stress-strain curve of the fiber-reinforced specimen (solid line) resembles that of a ductile material.

Table 3: Results and standard deviation of hand made specimen for fiber type evaluation. The abbreviation "aggl." in the following table stands for "agglomeration."

Number	Bend. strength [MPa]	Stddev[2] [MPa]	Emax[3] [%]	Stddev [%]	Bend. strength of ref. [MPa]	Emax of ref. [%]	Change of strength compared to ref. [%]	Change of Emax compared to ref. [%]	Mixing behaviour
GF1_1	2.12	0.43	0.10	0.01	3.29	0.09	–35.6	11.1	aggl. visible
GF2_1	4.66	0.16	0.11	0.00	5.85	0.12	–20.3	–8.3	no aggl.
GF2_2	5.27	0.24	0.12	0.01	5.85	0.12	–9.9	0.0	no aggl.
GF2_3	3.96	0.3	0.12	0.02	4.40	0.11	–10.0	9.1	no aggl.
GF2_4	4.85	0.32	0.15	0.01	5.85	0.12	–17.1	25.0	no aggl.
GF2_5	3.37	0.23	0.18	0.02	4.95	0.12	–31.9	50.0	no aggl.
GF2_6	4.38	0.6	0.22	0.03	5.85	0.12	–25.1	83.3	no aggl.[4]
GF2_7	3.25	0.35	0.14	0.02	4.17	0.11	–22.1	27.3	slight aggl.
GF2_8	1.01	0.15	0.16	0.05	3.60	0.11	–71.9	45.5	no aggl.[4]
GF2_9	4.04	0.35	0.11	0.01	6.71	0.11	–39.8	0.0	no aggl.
GF2_10	7.42	0.55	0.14	0.01	9.07	0.11	–18.2	27.3	no aggl.
GF3_1	4.02	0.46	0.25	0.04	4.95	0.12	–18.8	108.3	aggl. visible
GF4_1	0.87	0.22	0.2	0.03	3.60	0.11	–75.8	81.8	no aggl.
GF4_2	3.87	0.33	0.12	0.01	3.76	0.10	2.9	20.0	aggl. visible[5]
GF4_3	huge aggl., testing not possible								
GF5_1	4.24	0.13	0.11	0.01	4.33	0.11	–2.1	0.0	aggl. visible
GF5_2	3.63	0.41	0.10	0.01	4.33	0.11	–16.2	–9.1	aggl. visible
GF5_3	2.82	0.12	0.10	0.01	4.54	0.11	–37.9	–9.1	aggl. visible
GF6_1	4.28	0.41	0.13	0.00	4.97	0.1	–13.9	30.0	aggl. visible
GF6_2	3.63	0.51	0.13	0.01	4.97	0.1	–2.0	30.0	aggl. visible
GF7_1	1.02	0.09	0.1	0.02	2.35	0.06	–56.6	66.7	no aggl
GF7_2	1.3	0.32	0.12	0.02	2.35	0.06	–44.7	100.0	no aggl

Overall, it was observed that the addition of glass fibers generally leads to a decrease in breaking strength, with the exception of the GF4_2 mixture. However, the more significant factor is the change in elongation at break at F_{max}, which can be enhanced by increasing the amount of glass fibers, as depicted in *Figure 7*.

[2] standard deviation
[3] elongation at break
[4] Difficult to achieve a homogenous mixture.
[5] Big agglomerations were removed by hand.

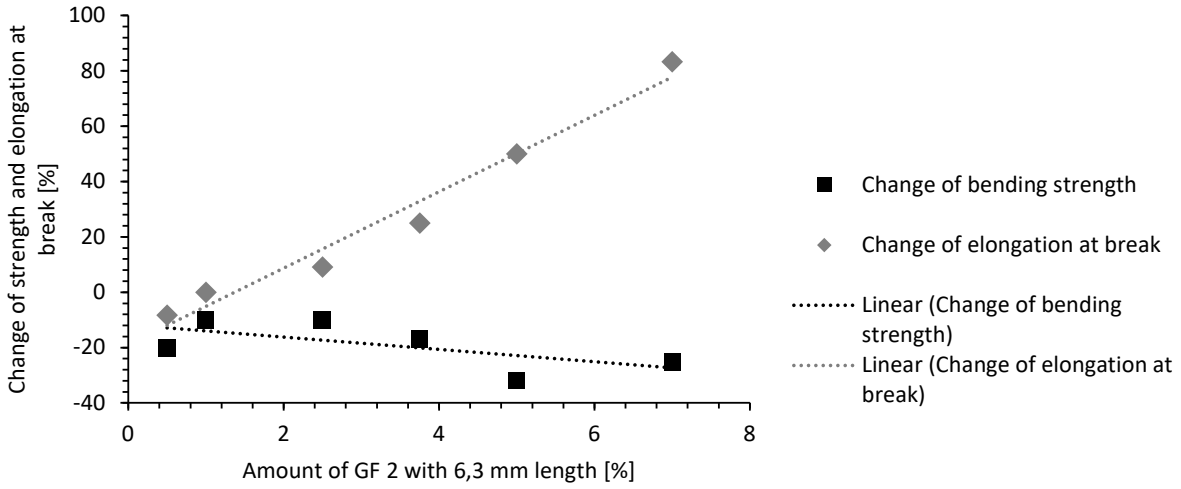

Figure 7: Influence of GF amount on bending strength and elongation at break compared to a reference without GF 2.

Increasing the amount of binder in the mixture enhances the bending strength (*Figure 8*); however, it does not significantly affect the elongation at break. Only the mixture containing 14 wt.% binder and 2.5 wt.% glass fibers resulted in a higher elongation at F_{max}, which can be seen in *Figure 9*.

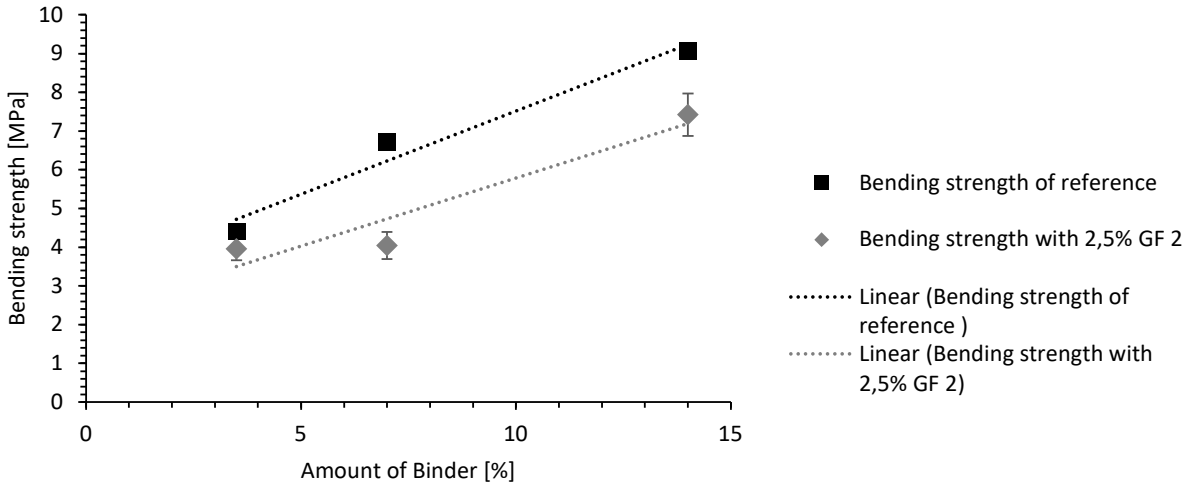

Figure 8: Influence of binder content on bending strength with and without GF 2.

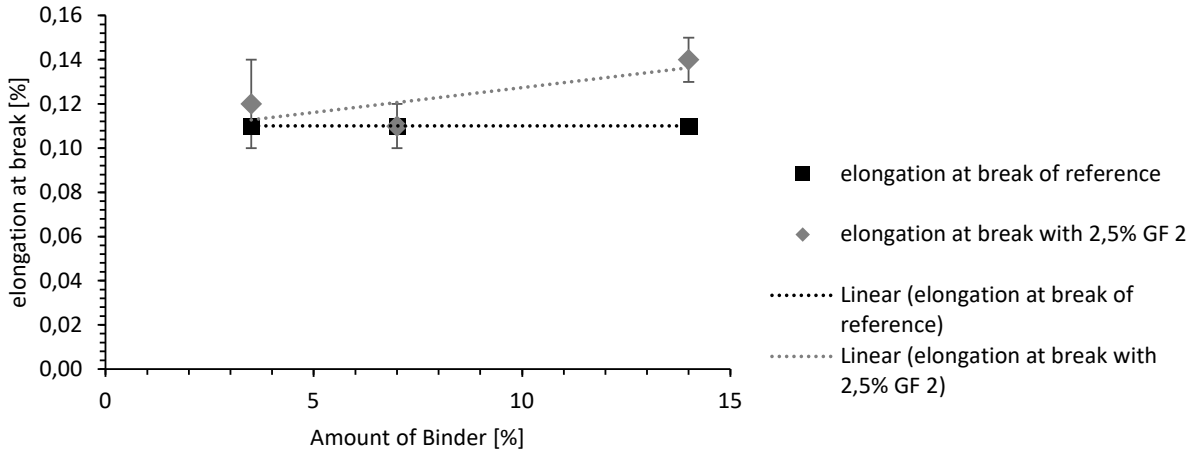

Figure 9: Influence of binder amount on elongation at break with and without GF 2.

Casting of Molds

Different fiber ratios within the casting mold obtained varying numbers of castings with different surface qualities. The criterion of failure was determined by considering the mold halves that were broken and could not be reused due to the casting process. At a fiber ratio of 3 wt.%, the casting molds were completely destroyed after the fourth casting. At fiber ratios of 5 wt.% and 7 wt.%, ten castings were obtained for each mold. However, the casting attempts were discontinued due to poor surface quality and not due to complete destruction of the casting mold. The reference molds without fiber reinforcement – produced in parallel to their respective fiber-reinforced casting molds – always broke after the first casting.

Table 4: Correlation between the fiber content within the casting mold and the achieved number of casts.

Fiber content within the casting mold	Achieved number of casts
0 wt.%	1
3 wt.%	4
5 wt.%	10
7 wt.%	10

The bending bars, produced in parallel to the casting molds, were tested in a 3-point bending test, as described in the "3-Point-Bending Test" chapter, to establish a correlation with the material's mechanical properties. *Figure 10* shows the evaluated results of the 3-point bending tests conducted on the bending bars produced in parallel to the casting molds containing different fiber amounts.

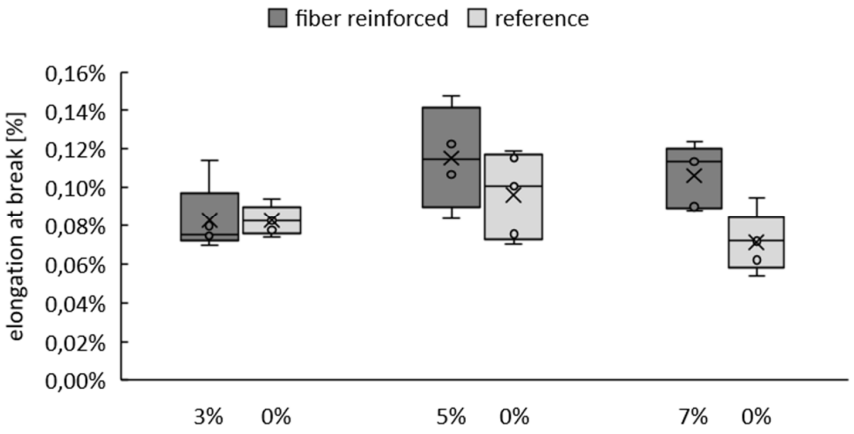

Figure 10: 3-point-bending test results of the respective five bending bars produced in parallel to the casting molds. The fiber-reinforced (varying fiber content 3 %, 5 % and 7 %) and reference (0 % fiber content) bending bars are compared.

During the measurement of the surface deviation of the castings from the original CAD file, only the casting series with 5 wt.% and 7 wt.% glass fiber content were considered because, in the casting experiment, a minimum of 10 castings could be produced in these series (*Table 4*). The results of this measurement are shown in *Figure 11*.

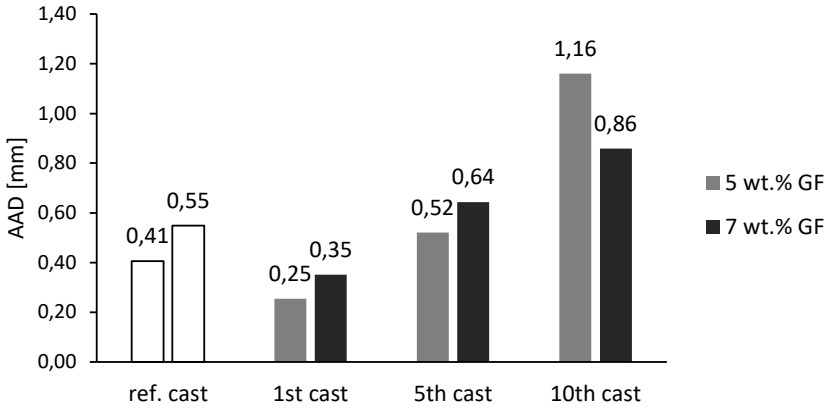

Figure 11: AAD[6] in relation to the number of castings. The reference castings (ref. cast) do not contain any fiber content and were depicted for the sake of comparison.

Multiple casting attempts were made per fiber content, however only one mold was used per fiber content. Therefore, only the trend can be observed, but the result is not statistically validated. The images generated using CloudCompare, which display the deviations of the individual casting from the designed form visually, are shown in *Figure 12*.

[6] Absolute Average Deviation

Cast	Casts made from fiber-reinforced mold with a fiber content of 5 wt.% (GF 2)	Casts made from fiber-reinforced mold with a fiber content of 7 wt.% (GF 2)
Ref. cast	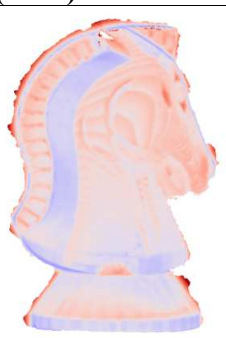	
1st cast		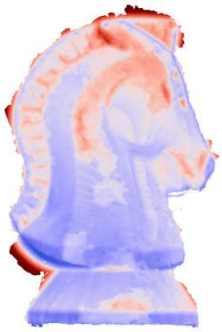
5th cast	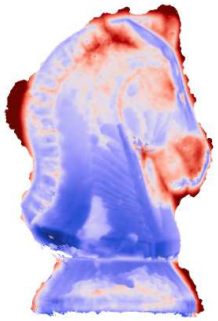	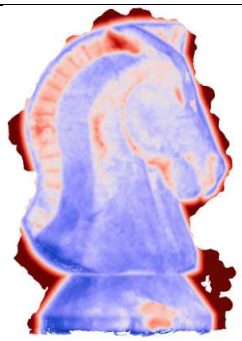
10th cast	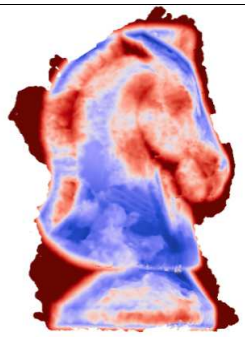	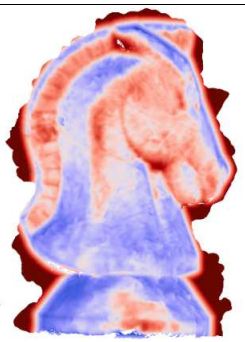

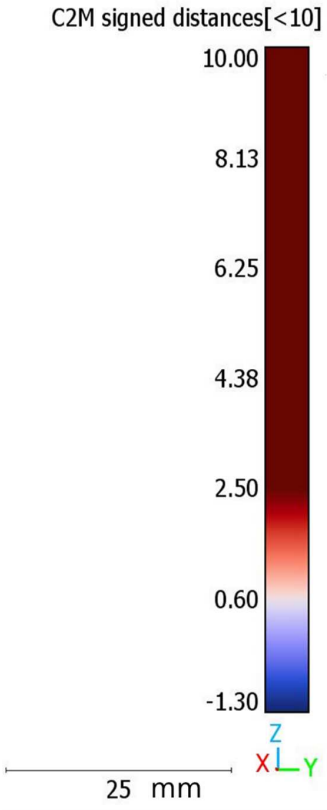

Figure 12: The deviations of the castings from the CAD file can be easily observed. With each casting attempt, the mold becomes more hollowed out, resulting in a greater deviation of the casting from the CAD file.

Binder-Jetting of Fiber-reinforced Bending Bars

The bending bars, which were produced using different binder systems and coating methods in the 3D-printing process, were tested in the 3-point bending test. The mechanical properties investigated included bending stress and elongation at break at maximum bending stress of the material system. In the organic 3D-printing experiment, two bending bars were produced, while in the inorganic 3D-printing experiment, three bending bars were produced. The evaluated test results are shown in *Figure 13*.

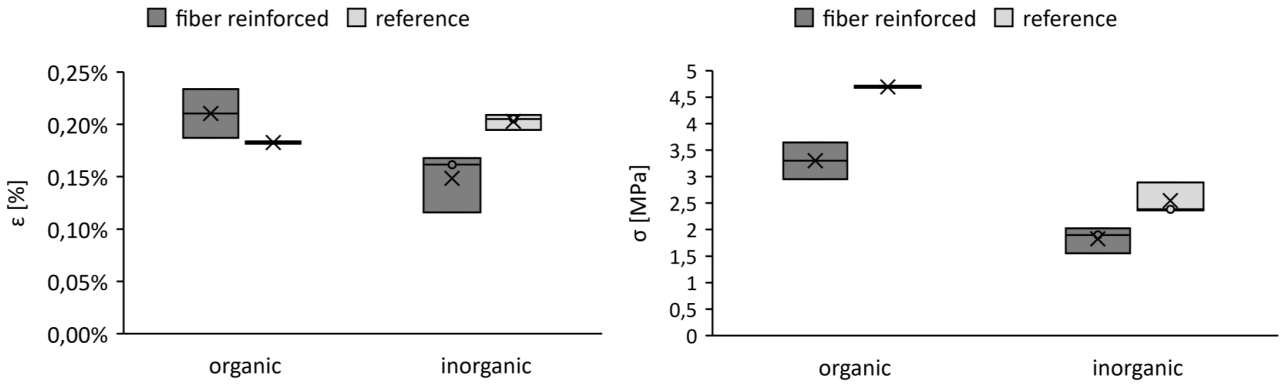

Figure 13: The left diagram shows the elongation at break at maximum stress. In the right diagram, the maximum stress is shown.

An image of the side view of a 3D-printed bending bar, manufactured using the organic binder system (RPT 2, *voxeljet AG*), GS14RP sand (*Strobel Quarzsand GmbH*), and 6.3 mm long GF2 glass fibers, can be seen in *Figure* 14. For the bending bars printed with the organic binder system, a roller coater, as described in "Materials and Methods", was used.

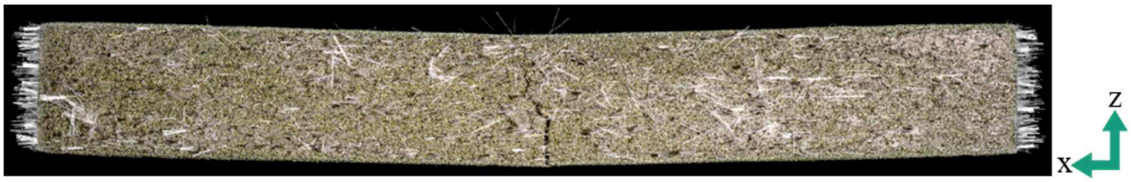

Figure 14: Organically in x-direction (see Figure 4) 3D-printed bending bar after the 3-point-bending test. The protruding glass fibers are clearly visible, as well as the fracture. The bending bar is still held together due to the presence of glass fibers.

Discussion

Specimen Production

For the selection of the right reinforcing fibers for the mold production, different glass fiber types were investigated regarding their reinforcing effect. The results are shown in detail in *Table 3*. It was found that GF 4 with 4.2 mm fiber length (uncoated glass fiber) was the best fiber regarding high bending strength, but a big drawback was the huge agglomeration of the uncoated fibers. A conducted pull-out test supports the theory, that the uncoated fibers are good as reinforcing fibers for inorganic binder systems since there is no sizing on the fibers which might lead to a poorer fiber-binder adhesion. The uncoated fibers are unfortunately not well miscible with sand and binder. This is the reason why fibers like GF 2 were investigated, too, here the mixing was easier and a homogenous mixing was possible. It was found that this type leads to a much higher elongation at break at F_{max} if enough fibers were used in the sand fiber mixture. The needed minimum amount of glass fiber for a higher elongation at break was 2.5 wt%, which can be seen in *Figure 7*. The use of a higher amount of binder did not lead to a higher elongation at break, which can be seen in *Figure 9*. Of all the fiber types studied, GF2 was the most suitable for mixing sand, fiber and binder, and was therefore studied in depth, and the required quantities of

this fiber for high flexural stress were researched in detail. These results were then used for mold production. In theory, recycled glass fibers (GF 7) could be used for this application, provided that it's feasible to mix these fibers and the recycled fibers are free from impurities on the surface. Milled glass fibers (GF 5) are not suitable, since they are too short to show the effect of creating a quasi-ductile breaking behavior. GF 1, GF 3, and GF 6 also showed agglomeration effects, so they were not further investigated. However, with a new mixing technology, those fibers might lead also to good results regarding the improvement in a higher elongation at F_{max}.

Casting of Molds and Surface Deviations

In *Figure 7*, we can see that the elongation at break increases with a higher proportion of glass fibers. Based on the casting experiments, we observed that a fiber-reinforced mold with a fiber content of 3 wt.% could only be used for four castings, while the fiber-reinforced molds with 5 wt.% and 7 wt.% could be used for at least ten castings. This suggests that the elongation at break has a decisive influence on the moldability of fiber-reinforced molds. The bending bars produced parallel to the casting molds do not show this strong dependency of elongation at break on the fiber content (*Figure 10*). This may be attributed to the manufacturing method of the bending bars. However, it can be claimed that fibers in the mold material enable multiple castings.

It was also observed that the fiber-reinforced molds exhibit increasing deviation from their original shape with each casting. This is likely due to the heat causing the water glass bonds in the top layer, adjacent to the melt, to decompose and release water, making the material system more brittle. This would support the hypothesis put forward by C. Appelt [20]. As a result, the top layer crumbles after each casting, leading to more erosion of the mold with each casting process.

This effect can also be observed in the images generated using GOM ATOS Compact Scan and the CloudCompare software, which can be seen in *Figure 12*. It can be clearly noticed that especially at sharp edges and corners, where the heat input of the melt is the highest, the hollowing phenomenon is also the most prominent. For example, in *Figure 12*, it can be seen that the casting flash significantly increases with each casting. Additionally, the details, such as the divisions of the mane of the knight, which are clearly visible in the first casting, become hardly noticeable in the tenth casting.

One possible way to slow down this process could potentially be the use of coatings that act as heat insulators between the melt and the fiber-reinforced mold. Furthermore, it is anticipated that a refractory coating would significantly improve the surface quality of the casting. The deviations from the ideal form could be reduced through centering. To better investigate the effects of thermal expansion on the mold, a more sophisticated model would be necessary. This needs to be further investigated in the next step.

Binder-Jetting of Fiber-reinforced Bending Bars

It could be demonstrated that GF 2 fibers can be processed in the 3D printing process using both binder systems (water glass and furan resin) and two different coating systems (roller and blade) with a layer thickness of 350 µm or more.

It is shown that with the 3D printing of fiber-reinforced bending bars using an organic binder system, a higher average elongation at break could be achieved compared to the reference bending bars without fiber reinforcement. It is also evident that the fiber-reinforced bending bars exhibit a quasi-ductile stress-strain behavior, which can be seen in the left diagram of *Figure 15*.

It is unclear why the 3D printed bending bars, printed with the inorganic binder, exhibit brittle fracture behavior, as seen in the right diagram in *Figure 15*. This could be due to the use of a different coating module used by the prototype in-house production 3D printer compared to the VX1000 3D printing system. The prototype 3D printer for the organic binder system spreads the sand onto the underlying sand layer that has already been sprinkled with glass fibers. It was observed that some of the fibers were still in a vertical position – possibly due to electrostatic forces – before the sand coating process. During the sand-spreading process, these vertical fibers were able to maintain their position and form a connection between the layers. By establishing fiber connections between the individual sand layers, the fibers can create a higher resistance to cracking, leading to a quasi-ductile material behavior. This could be a possible explanation for the quasi-ductile stress-strain behavior, which can be seen in the left diagram in *Figure 15*. Another possibility is that a too small quantity of fibers was introduced

through the manual process using a sieve. This would also result in the stress-strain curve shifting towards brittle failure. In further experiments, it is advisable to determine the quantity of fibers introduced to rule out this scenario.

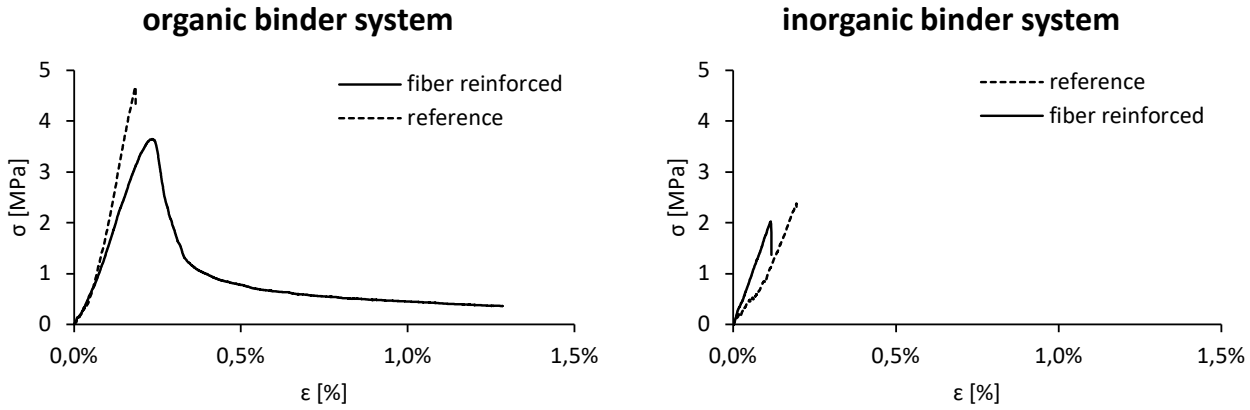

Figure 15: The left diagram shows the comparison of two representative stress-strain curves between a fiber-reinforced bending bar and a reference bending bar. The bending bars were 3D printed using an organic system. The right diagram displays the comparison of two representative stress-strain curves between a fiber-reinforced bending bar and a reference bending bar. The bending bars were 3D printed using an inorganic binder system.

In contrast, the stress-strain curves of the bending bars produced with an inorganic binder system showed a brittle behavior, regardless of whether they were fiber-reinforced or not. This can be seen in the right diagram of *Figure 15*. In this case, the fiber-reinforced bending bars also exhibited lower elongation compared to the reference bending bars. The average elongation at maximum bending stress was 0.15 % for the fiber-reinforced bending bars and 0.20 % for the reference bending bars. This was not expected. Again, the coating process could provide a possible answer. In the VX1000 3D printing system, the coating module dispenses sand from the front, which is then smoothed out with a blade. This sand wall created in front of the coating module smooths out all the fibers, including those that were in a vertical position. As a result, a pure layer of fibers is formed, sandwiched between two layers of sand. This does not allow for a connection between the sand layers through the fibers. The formation of these separate layers, sand-fiber-sand, prevents the fibers from providing resistance during crack formation. The sand layers fracture in a brittle manner, resulting in the failure of the entire bending bar.

It should be mentioned that three bending bars were produced with the inorganic binder system, while only two bending bars were produced with the organic binder system. Therefore, only a trend can be observed in this case as well. In order to statistically validate these results, further experiments are urgently needed. Furthermore, the glass fibers were manually sieved, so the exact amount of fibers per bending bar cannot be determined, and the amount of fibers introduced can vary greatly between the produced bending bars, which can also result in significant variation in the results of the 3-point bending test. This was also observed in the hand-formed bending bars. An amount of at least 3.75 wt.% glass fibers was necessary to observe a quasi-ductile material behavior in the fiber-reinforced bending bars.

Summary

Due to the continuous increase in sand consumption, a finite resource, it is desirable to guarantee resource-saving through further processing and reprocessing. To create an environmentally friendly and sustainable production chain in sand casting, new solutions for the binder systems and an efficient use of resources through reusable casting should be found. The aim of reinforcing sand molds and cores with fibers is to find a middle ground between the immense investment for permanent molds and the single use of sand molds.

It has been shown that the use of glass fibers generally reduces bending strength but increases elongation at break. This effect can be enhanced by increasing the addition of fibers. In summary, coated glass fibers (GF2)

with a length of 6.3 mm yielded the best results. Furthermore, it has been observed that a larger quantity of binder increases bending strength, but does not significantly alter elongation at break.

By adding glass fibers and thereby altering the material properties of the sand-binder system, bending beams with a quasi-ductile material behavior could be produced. This quasi-ductile material system is suitable for the production of sand molds for multiple castings, as demonstrated. Fiber-reinforced sand molds with a fiber content of 5 wt.% and 7 wt.% could withstand at least ten castings. It was observed that the mold was progressively damaged with each casting, but it did not completely break until the tenth casting. In contrast, reference molds consisting only of sand and binder without fiber content were completely destroyed after the first casting. There was a tendency that a higher fiber content allowed for a higher number of castings per mold, but this result still needs to be statistically validated.

The use of glass fibers was also demonstrated in the sand-based binder jetting process. Two different binder systems and coating processes were tested. It was shown that also in 3D printing the use of short fibers in combination with an organic binder system leads to a quasi-ductile behavior of the produced bending beams. Whether such a behavior can also be achieved with inorganic binder systems under modified process control is the subject of further investigations.

References

[1] R. Roller, V. Buck, Fachkunde Gießereitechnik: Technologie des Formens und Gießens, ninth., überarbeitete und erweiterte Auflage, Verlag Europa-Lehrmittel Nourney, Vollmer GmbH et Co. KG, Haan-Gruiten, 2021.

[2] H. Polzin, M. Mahn, Quarzsand aus Nobitz als Formgrundstoff für bentonitgebundene Formstoffe. https://www.giesserei-praxis.de/news-artikel/artikel/quarzsand-aus-nobitz-als-formgrundstoff-fuer-bentonitgebundene-formstoffe.

[3] P. Peduzzi, A. Vander Velpen, J. Lynggaard, S. Chuah, Global Sand Observatory Initiative. https://unepgrid.ch/en/activity/sand.

[4] D. Günther, R. Ramakrishnan, Rapid Prototyping von Sandformen mit anorganischen Bindersystemen (1. Phase), Friedberg / Garching, 2013.

[5] Philipp Lechner, A Material Model for Foundry Cores: The Brittle Fracture Behaviour of Chemically-Bound Foundry Sands, Technical University of Munich, 2021.

[6] B.J. Stauder, H. Kerber, P. Schumacher, Foundry sand core property assessment by 3-point bending test evaluation, Journal of Materials Processing Technology 237 (2016) 188–196. https://doi.org/10.1016/j.jmatprotec.2016.06.010.

[7] P. Lechner, G. Fuchs, C. Hartmann, F. Steinlehner, F. Ettemeyer, W. Volk, Acoustical and Optical Determination of Mechanical Properties of Inorganically-Bound Foundry Core Materials, Materials (Basel) 13 (2020). https://doi.org/10.3390/ma13112531.

[8] V. Afroughsabet, L. Biolzi, T. Ozbakkaloglu, High-performance fiber-reinforced concrete: a review, J Mater Sci 51 (2016) 6517–6551. https://doi.org/10.1007/s10853-016-9917-4.

[9] T. Ding, J. Xiao, S. Zou, J. Yu, Flexural properties of 3D printed fibre-reinforced concrete with recycled sand, Construction and Building Materials 288 (2021) 123077. https://doi.org/10.1016/j.conbuildmat.2021.123077.

[10] S. Adhikari, A. Patnaik, Potential applications of steel fibre reinforced concrete to improve seismic response of frame structures, 2012. https://www.researchgate.net/profile/anil-patnaik/publication/275893737_potential_applications_of_steel_fiber_reinforced_concrete_to_improve_seismic_response_of_frame_structures/links/554974610cf205bce7ac2fff/potential-applications-of-steel-fiber-reinforced-concrete-to-improve-seismic-response-of-frame-structures.pdf.

[11] R. Hajek, M. Foglar, A. Kohoutkova, Recent development in blast performance of fiber-reinforced concrete, IOP Conf. Ser.: Mater. Sci. Eng. 246 (2017) 12014. https://doi.org/10.1088/1757-899X/246/1/012014.

[12] H.-S. So, Spalling Prevention of High Performance Concrete at High Temperatures, in: S. Yilmaz, H.B. Ozmen (Eds.), High Performance Concrete Technology and Applications, InTech, 2016.
[13] B. Karasu, Glass fibre reinforced concrete (GFRC), 2018.
[14] H.M. Eldesouky, M.M. Morsy, M.F. Mansour, Fiber-reinforced sand strength and dilation characteristics, Ain Shams Engineering Journal 7 (2016) 517–526. https://doi.org/10.1016/j.asej.2015.06.003.
[15] K. Lü, X. Liu, Y. Lu, Z. Du, The interfacial characteristics and action mechanism of fibre-reinforced shell for investment casting, Int J Adv Manuf Technol 93 (2017) 2895–2902. https://doi.org/10.1007/s00170-017-0735-x.
[16] K. Lü, X. Liu, Z. Du, Y. Li, Properties of hybrid fibre reinforced shell for investment casting, Ceramics International 42 (2016) 15397–15404. https://doi.org/10.1016/j.ceramint.2016.06.188.
[17] P. Lechner, J. Stahl, F. Ettemeyer, B. Himmel, B. Tananau-Blumenschein, W. Volk, Fracture Statistics for Inorganically-Bound Core Materials, Materials (Basel) 11 (2018). https://doi.org/10.3390/ma11112306.
[18] H. Polzin, Anorganische Binder zur Form- und Kernherstellung in der Gießerei. Teilw. zugl.: Freiberg, TU Bergakad., Habil.-Schr., 2012, first. Aufl., Schiele & Schön, Berlin, 2012.
[19] F. Ettemeyer, M. Schweinefuß, P. Lechner, J. Stahl, T. Greß, J. Kaindl, L. Durach, W. Volk, D. Günther, Characterisation of the decoring behaviour of inorganically bound cast-in sand cores for light metal casting, Journal of Materials Processing Technology 296 (2021) 117201. https://doi.org/10.1016/j.jmatprotec.2021.117201.
[20] C. Appelt, Material properties and process requirements for inorganic core production, 2018.